

**DOI: 10.1103/PhysRevA.90.062704**

# Electron collisions with ammonia and formamide in the low- and intermediate-energy ranges

M. G. P. Homem,[1] I. Iga,[1] G. L. C. de Souza,[2] A. I. Zanelato,[3] L. E. Machado,[4] J. R. Ferraz,[4] A. S. dos Santos,[4] L. M. Brescansin,[5] R. R. Lucchese,[6] and M.-T. Lee[1]

[1]*Departamento de Química, UFSCar, 13565-905 São Carlos, SP, Brazil*
[2]*Departamento de Química, UFMT, 78060-900 Cuiabá, MT, Brazil*
[3]*Instituto de Ciências Exatas e Tecnologia, UFAM, 69100-000 Itacoatiara, AM, Brazil*
[4]*Departamento de Física, UFSCar, 13565-905 São Carlos, SP, Brazil*
[5]*Instituto de Física Gleb Wataghin, UNICAMP, 13083-970 Campinas, SP, Brazil*
[6]*Chemistry Department, Texas A&M University, College Station, Texas 77842-3012, USA*

(Received 27 October 2014; revised manuscript received 16 November 2014; published 2 December 2014)

We report an investigation on electron collisions with two nitrogen-containing compounds, namely ammonia ($NH_3$) and formamide ($NH_2CHO$). For ammonia, both theoretical and experimental differential, integral, and momentum-transfer cross sections, as well as calculated grand-total and total absorption cross sections, are reported in the 50–500 eV incident energy range. Calculated results of various cross sections are also reported for energies below 50 eV. Experimentally, angular distributions of the scattered electrons were measured using a crossed electron beam-molecular beam geometry and then converted to absolute differential cross sections using the relative flow technique. Absolute integral and momentum-transfer cross sections for elastic $e^-$-ammonia scattering were also derived from the measured differential cross sections. For formamide, only theoretical cross sections are presented in the 1–500 eV incident energy range. A single-center-expansion technique combined with the method of Padé was used in our calculations. For both targets, our calculated cross sections are compared with the present measured data and with the theoretical and experimental data available in the literature and show generally good agreement. Moreover, for formamide, two shape resonances located at 3.5 eV and 15 eV which correspond to the continuum $^2A''$ and $^2A'$ scattering symmetries, respectively, are identified. The former can be associated to the $^2B_1$ shape resonance in formaldehyde located at around 2.5 eV, whereas the latter can be related to the $^2E$ resonance in ammonia at about 10 eV. Such correspondence is very interesting and so supports the investigation on electron interaction with small building blocks, instead of with larger biomolecules.

DOI: 10.1103/PhysRevA.90.062704 PACS number(s): 34.80.Bm

## I. INTRODUCTION

Without any doubt, nitrogen-containing compounds constitute a class of most abundant and important materials in universe. These molecules have played an important role in the evolution of life on Earth. Recently, it has been discovered that significant damage to DNA and RNA, such as single or double strand breaks, can be caused by their interaction with low-energy electrons [1]. Large biomolecules are built from smaller components, most of them containing nitrogen. Thus electron interaction with such molecules which form building blocks of large biomolecules has attracted considerable attention in recent years [1,2]. In the near past, several small biomolecules such as methanol [3], ethanol [4], propane [5], and dimethylether [6] were investigated both theoretically and experimentally by our group. In this work, we present a study of electron collisions with two nitrogen-containing compounds, namely ammonia ($NH_3$) and formamide ($NH_2CHO$).

Electron scattering by ammonia has many practical applications in fields such as space physics, modeling of planetary atmospheres, gas-discharge lasers, switching devices, and plasma chemistry, where $NH_3$ is a source of nitrogen atoms for the fabrication of nitride films and other nitrogen-containing compounds [7]. In addition, due to the ozone-layer destruction by the chlorofluorocarbon compounds, ammonia has been reintroduced as a cooling gas, replacing the freons. Thus $e^-$-$NH_3$ interaction is also important in atmospheric studies, since the concentration of ammonia is expected to increase in Earth's atmosphere due to this replacement.

Previous experimental investigation on $e^-$-$NH_3$ scattering is limited. The very first experimental grand-total cross sections (TCS) were reported in the 1–20 eV energy range by Brüche [8] in 1929. Lately, TCS were also measured by Sueoka *et al.* [9] using a time-of-flight technique and by Szmytkowski *et al.* [10], Zecca *et al.* [11], and García and Manero [12] using a linear transmission technique. More recently, experimental TCS were reported by Ariyasingue *et al.* [13] in the 400–4000 eV range and by Jones *et al.* [14] in the 0.02–10 eV range. Also, experimental total ionization cross sections (TICS) were reported by Rao and Srivastava [15]. In addition, Hayashi [16] reported momentum-transfer cross sections (MTCS) which are based on the drift velocity measurements of Pack *et al.* [17] and the calculations of Altshuler [18]. Absolute elastic differential cross sections (DCS) at 7.5 eV energy were reported by Ben Arfa and Tronc [19] and also relative DCS were reported by Furlan *et al.* [20] in the 12–50 eV range. The most complete experimental DCS determination for this target was probably that performed by Alle *et al.* [21]. In that work, absolute DCS were reported in the 2–30 eV energy range and in the 10°–125° angular range. Above 30 eV, the only set of experimental DCS in absolute scale were those of Bromberg measured in the 2°–10° angular range and at incident energies of 300, 400, and 500 eV, reported in the article of Harshbarger *et al.* [22]. Relative DCS, measured in the same energy and angular ranges but normalized to those of Bromberg, were also reported by Harshbarger *et al.* [22]. Finally, absolute measurements of DCS for the electron impact excitation of the $\nu_{1,3}$ vibrational

 

modes of $e^-$-$NH_3$ at incident energies of 5, 7.5, and 15 eV were reported by Gulley *et al.* [23].

From the theoretical point of view, the literature for the elastic scattering of electrons by $NH_3$ is quite abundant. Some earlier DCS calculations include those reported by Gianturco and Jain [24], Pritchard *et al.* [25], Gianturco [26], and Rescigno *et al.* [27]. More recently, calculations were also reported by Ribeiro *et al.* [28] and by Munjal and Baluja [29]. In all these calculations, the framework of the fixed-nuclei approximation combined with the single-center expansion technique was employed. This procedure may cause severe convergence problems in the calculation of electron-polar molecule cross sections due to truncations in partial-wave expansions [25]. Because of that, Pritchard *et al.* reported DCS only at intermediate and backward angles where the first few partial waves dominate the description of the interaction dynamics. On the other hand, Gianturco [26], Rescigno *et al.* [27], and Munjal and Baluja [29] applied the Born-closure method to overcome this difficulty. Nevertheless, these calculations were limited to incident energies up to 20 eV. At higher energies, elastic DCS in the 0.1–1.0 keV range were calculated by Jain *et al.* using a parameter-free spherical optical potential at the static-exchange-polarization (SEP) level of approximation. In addition, calculations of TCS [31–33] and TICS [31] are also available in the literature.

Formamide, a derivative of ammonia, constitutes the simplest molecular system containing the peptide bond. Since the peptide type of chemical bonds are essential in the structure of proteins, the investigation on electron interaction with formamide can be useful to understand processes of electron-protein interactions and modeling of energy deposition upon high-energy irradiation of biomaterials [34]. Moreover, formamide is also considered as a prebiotic molecule. The identification of this system in the interestellar regions [35] has stimulated considerable studies in the astrobiological research in recent years. Despite that, the investigation on $e^-$-formamide interaction reported in the literature is very limited, both theoretically and experimentally.

Theoretical integral cross sections (ICS) and MTCS for elastic scattering of low-energy electrons (1–12 eV) by this target were calculated by Bettega [36] using the Schwinger multichannel method (SMC). The elastic DCS, ICS, and MTCS and the excitation cross sections from the ground state to the first four low-lying electron excited states at incident energies up to 10 eV were recently calculated by Wang and Tian [37] using the *R*-matrix method. In addition, TICS in the 10–2000 eV range were calculated by Gupta *et al.* [38] using the spherical complex optical potential (SCOP) approach.

Experimentally, absolute DCS for elastic $e^-$-$NH_2CHO$ scattering were measured and reported by Maljković *et al.* [34] at 100, 150, and 300 eV energies and in the 20°–110° angular range. To our knowledge, no other theoretical and/or experimental determinations of cross sections for this system were reported.

In this work, we present a joint theoretical-experimental study of electron scattering by ammonia in the low- and intermediate-energy ranges. Also, a theoretical investigation on $e^-$-$NH_2CHO$ collisions is reported. Specifically, experimental absolute DCS for electrons elastically scattered from $NH_3$ are determined using the relative flow technique (RFT) [39] in the 50–500 eV range and in the 10°–130° angular range. ICS and MTCS are also derived from the experimental DCS. Theoretically, DCS, ICS, MTCS, TCS, and total absorption cross sections (TACS) are also reported in 1–500 eV energy range for both ammonia and formamide. Thus the present study represents an attempt to partially fill the lack of both theoretical and experimental results for $e^-$-$NH_3$ and $e^-$-$NH_2CHO$ collisions.

The organization of this work is as follows. In Sec. II, we present some details of our experimental procedure. In Sec. III, the theory is briefly described. In Sec. IV, some computational details are presented and our calculated results for ammonia and formamide are compared with the present measured results, as well as with existing experimental and theoretical data. Some concluding remarks are also presented in Sec. V.

## II. EXPERIMENTAL PROCEDURE

The experimental setup and procedure used in the present measurement are given in detail in some of our previous works [40,41]. Briefly, the relative angular distribution of the scattered electrons at a given incident electron energy is measured using a crossed electron beam-molecular beam geometry. The scattered electrons are energy filtered by a retarding-field energy selector with a resolution of about 1.5 eV. This resolution allows the discrimination of inelastically scattered electrons that resulted from electronic excitation, whereas those from vibrational excitation processes remain unresolved. Thus our measured DCS are indeed vibrationally summed.

The sample of ammonia used in the measurements is prepared in our laboratory from a commercial ammonia solution with concentration of 36% in weight. For each measurement, a sample of ammonia solution is put into a glass balloon attached to a gas handling manifold and then undergoes a pretreatment for elimination of atmospheric air, through several freeze-thaw cycles using liquid nitrogen as the cooling agent. After these steps, the balloon with the liquid sample is then immerged into a Dewar frask filled with ice and salt. The temperature of this system is around $-20\,^{\circ}$C. At such low temperature, the vapor pressure of water is negligible compared to that of ammonia. In fact, the purity of the gaseous ammonia so generated was constantly checked using both a quadrupole mass spectrometer and a time-of-flight mass spectrometer [42], and was shown to be better than 99%. During the measurements, the working pressure in the vacuum chamber was around $5\times10^{-7}$ torr.

The recorded scattering intensities were converted into absolute elastic DCS using the RFT [39]. Accordingly, the DCS for a gas under determination ($x$) can be related with the known DCS of a secondary standard ($std$) as

$$\left(\frac{d\sigma}{d\Omega}\right)_x = \left(\frac{d\sigma}{d\Omega}\right)_{std} \frac{I_x}{I_{std}} \frac{R_{std}}{R_x} \left(\frac{M_{std}}{M_x}\right)^{\frac{1}{2}}, \qquad (1)$$

where $I$ is the scattered electron intensity, $R$ is the relative flow rate, and $M$ is the molecular weight. The application of RFT requires precise measurements of $R$ for both gases, $x$ and $std$. They were determined according to the procedure described in our previous studies [3,4,43].

In the present study, the absolute DCS of Ar and $N_2$ reported by Jansen *et al.* [44] and Dubois and Rudd [45] were used as secondary standards. Details of the analysis of the experimental uncertainties have also been given elsewhere [40,41]. They were briefly estimated as follows. Uncertainties of random nature such as pressure fluctuations, electron-beam current readings, background scattering, etc., were estimated to be less than 2%. These contributions combined with the estimated statistical errors gave an overall uncertainty of 4% in the relative DCS for each gas. Also, the experimental uncertainty associated with the normalization procedure was estimated to be 5.7%. These errors combined with the quoted errors [45] in the absolute DCS of the secondary standard provided an overall experimental uncertainty of 15% in our absolute DCS. Absolute DCS were determined in the 10°–130° angular range. In order to obtain ICS and MTCS, a manual extrapolation procedure was adopted to estimate DCS at scattering angles out of the angular range covered experimentally. The overall uncertainties on the ICS and MTCS were estimated to be 24%.

## III. THEORY

The theory used in this work is essentially the same as in several previous works [5,46,47]. Briefly, a complex optical potential given by

$$V_{opt} = V_{st} + V_{ex} + V_{cp} + i\,V_{ab} \tag{2}$$

was used to represent the electron-target interaction. Using this optical potential, the many-body nature of the electron-molecule interaction is reduced to a one-particle scattering problem which can be solved exactly using the numerical solution of the close-coupling Lippmann-Schwinger (LS) integral equation. In the above equation, $V_{st}$ and $V_{ex}$ are the static and the exchange components, respectively, and $V_{cp}$ is the correlation-polarization contribution. In addition, $V_{ab}$ is an absorption potential which describes the reduction of the flux of elastically scattered electrons due to opening of inelastic scattering channels.

The reduced form of the optical potential $U_{opt} = 2V_{opt}$ can be partitioned as a sum of two components:

$$U_{opt} = U_1 + U_2, \tag{3}$$

with

$$U_1 = U_{st} + U_{ex}^{loc} + U_{cp} \tag{4}$$

and

$$U_2 = U_{ex} - U_{ex}^{loc} + i\,U_{ab}, \tag{5}$$

where $U_{ex}^{loc}$ is a reduced local exchange potential. According to the two-potential formalism, the full transition $T$ matrix, given as

$$T_{fi} = \langle \phi(\vec{k}_f)|U_{opt}|\psi^+(\vec{k}_i)\rangle, \tag{6}$$

is also composed of two parts:

$$T_{fi} = T_1 + T_2, \tag{7}$$

where

$$T_1 = \langle \phi(\vec{k}_f)|U_1|\psi_1^+(\vec{k}_i)\rangle \tag{8}$$

and

$$T_2 = \langle \psi_1^-(\vec{k}_f)|U_2|\psi^+(\vec{k}_i)\rangle. \tag{9}$$

In Eqs. (6) and (8), $\phi$ is the unperturbed plane wave, $\psi$ is the solution of the LS equation for the full optical potential $U_{opt}$, $\psi_1$ is the solution of the distorted-wave LS equation for potential $U_1$, and $k$ is the magnitude of the electron linear momentum.

Further, $T_2$ can be obtained iteratively using the $[N/N]$ technique of Padé [48]:

$$T_2[N/N] = -\sum_{i,j=1,N-1} \langle \psi_1^-|U_2|\phi^{(i)+}\rangle (D^{-1})_{ij} \langle \phi^{(j)-}|U_2|\psi_1^+\rangle, \tag{10}$$

where

$$D_{ij} = \langle \phi^{(i)-}|U_2 - U_2 G_1^+ U_2|\phi^{(j)+}\rangle, \tag{11}$$

and $G_1$ is the distorted-wave Green's function, which satisfies the following condition:

$$(\nabla^2 + k^2 - U_1)G_1^{\pm}(\vec{r},\vec{r}') = \delta(\vec{r},\vec{r}'). \tag{12}$$

The superscripts $-$ and $+$ appearing in the above equations denote the incoming- and outgoing-boundary conditions of the scattering waves, respectively. In our calculation, the truncation parameter $N$ is iteratively increased until convergence is achieved. The converged body-frame (BF) $T$ matrix (or equivalently the BF scattering amplitude $f$) can then be expressed in the laboratory frame (LF) by the usual frame transformation [49]. Additionally, the TCS for electron-molecule scattering are obtained using the optical theorem:

$$\sigma_{tot} = \frac{4\pi}{k}\mathrm{Im}[f(\theta = 0^\circ)]. \tag{13}$$

In the present work, $U_{st}$ and $U_{ex}$ were derived exactly from a near-Hartree-Fock self-consistent-field (HF-SCF) target wave function, whereas $U_{cp}$ was obtained in the framework of the free-electron-gas model, derived from a parameter-free local density, as prescribed by Padial and Norcross [50], and the absorption potential $U_{ab}$ in Eq. (5) was the reduced scaled quasifree scattering model (SQFSM) absorption potential of Lee *et al.* [51], which is an improvement of the version 3 of the model absorption potential originally proposed by Staszewska *et al.* [52]. The Hara free-electron-gas-exchange potential [53] was used to generate the local exchange potential $U_{ex}^{loc}$.

## IV. COMPUTATIONAL DETAILS AND RESULTS

### A. Ammonia

The HF-SCF wave function of ammonia was obtained using the aug-cc-pVTZ (6D,10F) basis set of the GAUSSIAN 03 package [54]. At the experimental ground-state molecular geometry [55], this basis provided a total energy of −56.221 023 hartrees. The calculated electric dipole moment was 1.4682 D, in good agreement with the experimental value of 1.470 D [55]. Moreover, the asymptotic form of $U_{cp}$ was generated with the dipole polarizabilities [55] calculated at the HF-SCF level using the same basis set. The obtained values were $\alpha_{xx} =$ 12.31 a.u., $\alpha_{yy} = 12.31$ a.u., and $\alpha_{zz} = 12.80$ a.u., resulting

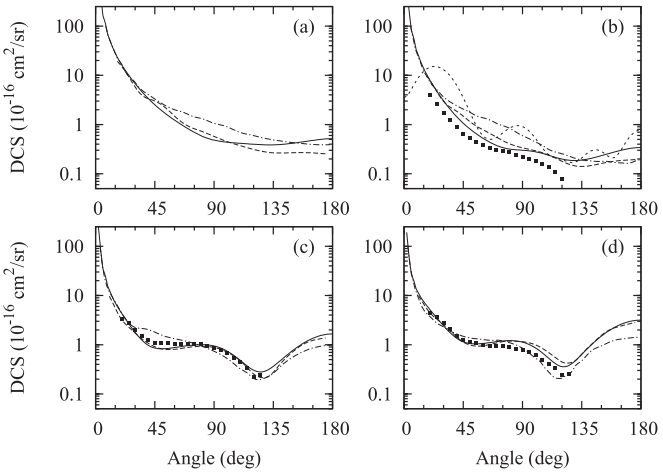


FIG. 1. DCS for elastic $e^-$-ammonia scattering at (a) 1 eV, (b) 2 eV, (c) 5 eV, and (d) 7.5 eV. Full curve, present theoretical results calculated with Born-closure procedure; dashed curve, calculated data of Rescigno *et al.* [27]; dashed-dotted curve, calculated data of Munjal and Baluja [29]; short-dashed curve, present theoretical results calculated without Born-closure procedure; solid squares, measured data of Alle *et al.* [21].

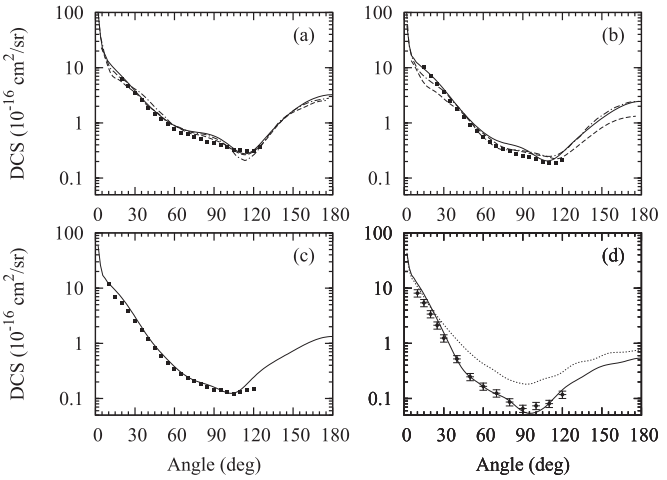


FIG. 2. Same as Fig. 1 but at (a) 15 eV, (b) 20 eV, (c) 30 eV, and (d) 50 eV except: dotted curve, present theoretical results calculated without inclusion of absorption effects; solid circles with error bars, present experimental data.

in an average dipole polarizability of $\alpha_0 = 12.473$ a.u., in fair agreement with the experimental value of 14.192 a.u. [55]. In our calculation, the wave functions and the interaction potentials, as well as the related matrices, were single-center expanded about the center of mass of the molecule in terms of the well known $X_{lh}^{p\mu}$ symmetry-adapted functions [56]. The truncation parameters used in these expansions were $l_c = 25$ and $h_c = 25$ for all bound and continuum orbitals, as well as for the $T$-matrix elements. The calculated cross sections were converged with $N = 7$. Since ammonia is a polar system, the partial-wave expansions converge slowly due to the long-range nature of the dipole interaction potential. In order to overcome this difficulty, a Born-closure formula was used to account for the contribution of higher partial-wave components to the scattering amplitudes. The procedure used was the same as in some of our previous studies [4,57,58].

The comparison of the present experimental and calculated DCS data with the existing theoretical [27,29] and measured [21] results is made in Figs. 1–3. In Fig. 1, our theoretical dipole-Born-corrected DCS for elastic electron scattering by ammonia in the 1–7.5 eV range are presented. Particularly, in Fig. 1(b), DCS obtained without a dipole-Born correction at 2 eV are also shown. It is seen that our DCS calculated without the dipole-Born correction present unphysical oscillations, due to the lack of convergence of the partial-wave expansion. Also, in this low-energy range, absorption effects were not included in the present study and, therefore, our calculations were performed at the same level of approximation as those of Rescigno *et al.* [27] and Munjal and Baluja [29]. From Fig. 1, it is seen that our calculated results are in good agreement with the experimental DCS of Alle *et al.* [21]. Comparing with other theoretical results, it is seen that at 5 and 7.5 eV, there is a general good agreement among all the calculated DCS. Nevertheless, at 1 and 2 eV, there are some discrepancies between these results, particularly at scattering angles larger than 40°. In general, our results are in better agreement with those of Rescigno *et al.* [27].

In Figs. 2 and 3, we present our theoretical dipole-Born-corrected DCS for elastic electron scattering by ammonia in the 15–500 eV energy range. In this range, the absorption effects were taken into account in our calculations. At 15 and 20 eV, comparison is made with the theoretical results of Rescigno *et al.* [27] and Munjal and Baluja [29]. Very good agreement is also seen among all these theoretical results which seems to indicate that the absorption effects are still weak at these energies. Nevertheless, above 30 eV inelastic scattering processes become relevant and thus affect significantly the elastic scattering processes. Such influences are clearly seen in Figs. 2(d) and 3(a), where DCS at 50 and 100 eV calculated without inclusion of absorption effects are also shown. It is seen that the DCS calculated without

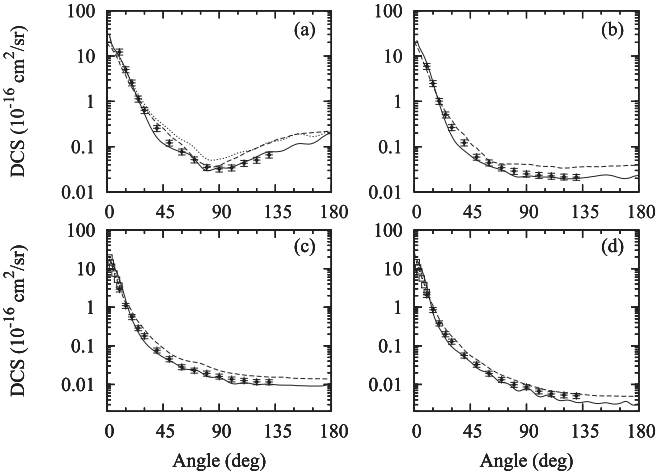


FIG. 3. Same as Fig. 2 but at (a) 100 eV, (b) 200 eV, (c) 300 eV, and (d) 500 eV, except: dashed line, calculated SHP1 results of Jain *et al.* [30] using the SCOP model; open squares, experimental DCS of Bromberg [22].

such effects lie significantly above those including them. In addition, our theoretical results are also compared with the experimental data of Alle *et al.* [21] at energies up to 30 eV and with the present measured data in the 50–500 eV range. There is a very good agreement between our theoretical data calculated with absorption effects and both experimental data. At 300 and 500 eV, the experimental DCS of Bromberg measured in the 2°–10° angular range [22] are also shown. These results seem to match very well to our measured data. At the only overlapping scattering angle, 10°, the results of Bromberg and our data agree within the experimental uncertainties at incident energies of 400 and 500 eV. However, his DCS at 10° and 300 eV is slightly out of the uncertainty margin. At these energies, our calculated results also agree well with both the present measured data and with those of Bromberg [22], although some small oscillations are seen in our theoretical DCS, particularly at scattering angles larger than 60°. Such oscillations are not clear in the experimental data and can be attributed to the lack of higher partial waves in the expansion of both the interaction potential and the $T$-matrix elements.

Figures 4(a) and 4(b) show our theoretical elastic ICS and MTCS, respectively, in the 1–500 eV energy range. Our ICS are compared with the calculated results of Munjal and Baluja [29] at energies up to 20 eV, with the experimental results of Alle *et al.* [21] in the 2–30 eV energy range, and with the present experimental ICS in the 50–500 eV range. Since at energies below the electronic excitation threshold the ICS and the TCS are essentially equivalent, the experimental TCS data of Jones *et al.* [14] at energies up to 10 eV are also shown. Our calculated ICS show a strong enhancement towards zero energy, which is due to the large target dipole moment. This feature is also seen in the theoretical ICS of Munjal and Baluja, and confirmed by the experimental TCS of Jones *et al.* Moreover, a broad resonance feature, centered at about 10 eV is seen, in agreement with the experimental results of Alle *et al.* [21]. Both the partial ICS and eigenphase-sum analyses indicated that the observed feature is a shape resonance in the continuum $^2E$ scattering channel. Quantitatively, our calculated results are in fair agreement with the TCS of Jones *et al.* at the overlapping energies. The experimental results of Alle *et al.* agree well with our calculated data in the 5–30 eV range, but lie well below our data at 2 eV. This disagreement is not surprising, since their experimental ICS were generated by integrating the DCS, which are extrapolated to the angular region where the DCS are strongly peaked, specially at such low incident energies. At energies of 50 eV and above, there is a very good agreement between our calculated and experimental ICS.

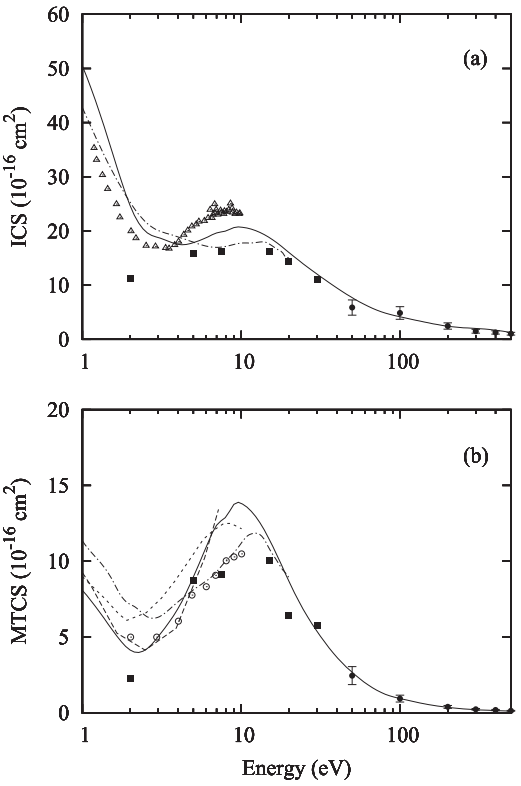


FIG. 4. (a) ICS and (b) MTCS for elastic $e^-$-ammonia scattering in the 1–500 eV range. Full curve, present dipole-Born-corrected results; dashed-dotted curve, calculated data of Munjal and Baluja [29]; dashed curve, calculated MTCS of Rescigno *et al.* [27]; short-dashed curve, calculated MTCS of Gianturco [26]; full circles with error bars, present experimental data; solid squares, experimental data of Alle *et al.* [21]; open triangles, experimental TCS of Jones *et al.* [14]; open circles, recommended MTCS of Itikawa [59].

In Fig. 4(b), our calculated MTCS are compared with the experimental data of Alle *et al.* [21] in the 2–30 eV range, with the present experimental MTCS in the 50–500 eV range, and also with the recommended data of Itikawa [59]. The calculated MTCS of Gianturco [26], Rescigno *et al.* [27], and Munjal and Baluja [29] are also shown for comparison. Our calculated data agree very well with the present experimental data. At lower energies, our MTCS agree reasonably well with the experimental results of Alle *et al.* and with the recommended data of Itikawa. Comparison with other theoretical data also shows good agreement, particularly with those of Rescigno *et al.* [27].

In Fig. 5(a) we show our calculated TCS for electron scattering by ammonia in the 1–500 eV range. Our TCS are compared with the experimental data of Jones *et al.* [14], Szmytkowski *et al.* [10], Zecca *et al.* [11], and with the calculated data of Limbachiya *et al.* [33]. At 7 eV and above, our calculated TCS agree very well with the experimental data of Szmytkowski *et al.* and Zecca *et al.* At lower energies, our data are in reasonably good agreement with the experimental results of Jones *et al.* [14]. Although the measured data of Szmytkowski *et al.* [10] show a similar trend towards zero incident energy, they are significantly underestimated in this region. Comparison with the theoretical results of Limbachiya *et al.* [33] shows good agreement with our TCS at energies above 20 eV. At lower energies, their results are substantially underestimated. This discrepancy can be attributed to the fact that no Born-closure correction was included in their calculations. In Fig. 5(b), our TACS are compared with the experimental TICS of Rao and Srivastava [15], and with the calculated TICS of Joshipura *et al.* [31] using the SCOP model and also with the present TICS calculated using the binary-encounter Bethe (BEB) model [60]. Our TACS agree qualitatively with the experimental and calculated TICS. Quantitatively, our TACS are systematically larger than all

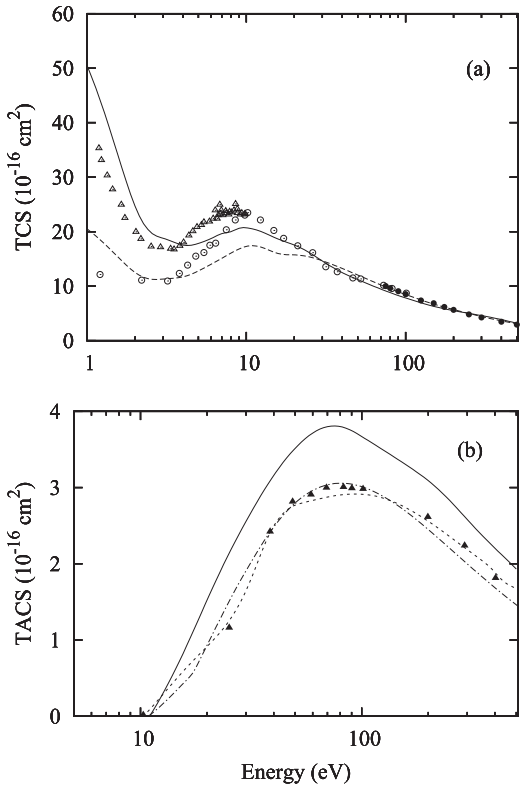


FIG. 5. (a) TCS and (b) TACS for $e^-$-ammonia scattering. Full curves, present calculated data; dashed curve, calculated results of Limbachiya *et al.* [33]; open triangles, experimental TCS of Jones *et al.* [14]; open circles, measured data of Szmytkowski *et al.* [10]; full circles, experimental TCS of Zecca *et al.* [11]; short-dashed curve, calculated TICS of Joshipura *et al.* [31]; dashed-dotted curve, present theoretical TICS calculated using the BEB model; full triangles, experimental TICS of Rao and Srivastava [15].

the TICS. These results are expected, since TACS account for all inelastic scattering processes including excitation and ionization, whereas only ionization processes are accounted for in the TICS.

For completeness, our experimental data of DCS, ICS, and MTCS, obtained in the 50–500 eV energy range, are presented in Table I.

### B. Formamide

The HF-SCF wave function of formamide was obtained using the double-zeta-valence (DZV) basis of the GAMESS package [61] and using the polarization of HONDO7. The calculation was performed at the experimental ground-state molecular geometry of this target [55]. The obtained electric dipole moment was 4.248 D, which agrees well with the calculated value of 4.28 D of Bettega *et al.* [36] and is also in fairly good agreement with the experimental value of 3.73 D [55]. The calculated dipole polarizabilities were $\alpha_{xx} = 24.940$ a.u., $\alpha_{yy} = 19.21$ a.u., and $\alpha_{zz} = 9.37$ a.u., which were used to generate the asymptotic form of $U_{cp}$. For this target, the truncation parameters used in the single-center expansion of the bound and scattering wave functions, the interaction potentials, and all the related matrices were $l_c = 35$ and $h_c = 35$. The calculated cross sections were converged with $N = 7$. Also for formamide, a Born-closure correction was applied to account for the contribution of higher partial-wave components to the scattering amplitudes. The procedure used is the same as for ammonia.

In Fig. 6, we compare our calculated DCS for elastic $e^-$-$NH_2CHO$ scattering with the theoretical data of Wang and Tian [37] in the 2–10 eV energy range. This comparison shows fair agreement between the data calculated using the different theoretical methods, particularly at 6 eV and 10 eV. Moreover, some oscillations in the calculated results might be unphysical and are probably an artifact of the Born-closure procedure [62].

TABLE I. Experimental DCS (in $10^{-16}$ cm$^2$/sr), ICS, and MTCS (in $10^{-16}$ cm$^2$) for elastic $e^-$-ammonia scattering. Note: 1.23(1) means $1.23 \times 10^1$.

| Angle | $E$ (eV) | | | | | |
|---|---|---|---|---|---|---|
| (deg) | 50 | 100 | 200 | 300 | 400 | 500 |
| 10 | 8.11(0) | 1.23(1) | 5.96(0) | 2.92(0) | 2.75(0) | 2.11(0) |
| 15 | 5.41(0) | 5.03(0) | 2.49(0) | 1.10(0) | 9.88(−1) | 8.59(−1) |
| 20 | 3.39(0) | 2.57(0) | 1.01(0) | 5.61(−1) | 4.87(−1) | 3.86(−1) |
| 25 | 2.12(0) | 1.13(0) | 5.09(−1) | 2.89(−1) | 2.44(−1) | 2.02(−1) |
| 30 | 1.24(0) | 6.33(−1) | 2.66(−1) | 1.80(−1) | 1.62(−1) | 1.29(−1) |
| 40 | 5.22(−1) | 2.53(−1) | 1.22(−1) | 7.64(−2) | 6.90(−2) | 5.66(−2) |
| 50 | 2.47(−1) | 1.21(−1) | 5.92(−2) | 4.55(−2) | 4.08(−2) | 3.28(−2) |
| 60 | 1.66(−1) | 7.73(−2) | 4.42(−2) | 2.82(−2) | 2.52(−2) | 1.92(−2) |
| 70 | 1.25(−1) | 5.18(−2) | 3.44(−2) | 2.30(−2) | 1.89(−2) | 1.33(−2) |
| 80 | 8.63(−2) | 3.49(−2) | 2.90(−2) | 1.93(−2) | 1.36(−2) | 9.86(−3) |
| 90 | 6.59(−2) | 3.24(−2) | 2.51(−2) | 1.61(−2) | 1.11(−2) | 8.57(−3) |
| 100 | 7.39(−2) | 3.42(−2) | 2.35(−2) | 1.36(−2) | 9.62(−3) | 6.70(−3) |
| 110 | 8.09(−2) | 4.32(−2) | 2.26(−2) | 1.25(−2) | 9.12(−3) | 5.66(−3) |
| 120 | 1.18(−1) | 5.06(−2) | 2.16(−2) | 1.15(−2) | 8.71(−3) | 5.28(−3) |
| 130 | | 6.62(−2) | 2.12(−2) | 1.14(−2) | 8.13(−3) | 5.06(−3) |
| ICS | 5.87(0) | 4.86(0) | 2.46(0) | 1.50(0) | 1.26(0) | 1.05(0) |
| MTCS | 2.45(0) | 9.90(−1) | 3.87(−1) | 2.26(−1) | 1.77(−1) | 1.27(−1) |

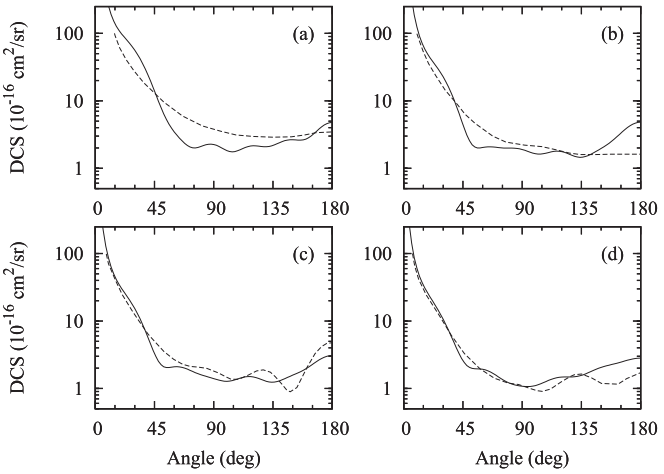


FIG. 6. Theoretical DCS for elastic $e^-$-$NH_2CHO$ scattering at (a) 2 eV, (b) 4 eV (c) 6 eV, and (d) 10 eV. Full curve, present results; dashed curve, calculated data of Wang and Tian [37] using the $R$-matrix method.

In Fig. 7, the calculated data in the 100–300 eV range are presented. The experimental DCS of Maljković *et al.* [34] measured at 100, 150, and 300 eV are also presented for comparison. It is seen that there is a good agreement between theory and experiment, except that some small oscillations seen in the theoretical results are not clear in the measured data. Nevertheless, we believe that those oscillations are physical and can be attributed to electron-diffraction effects.

In Figs. 8(a) and 8(b) we present the calculated ICS and MTCS, respectively, for this system. We have identified two shape resonances: the one located at about 3.5 eV is a resonance in the $^2A''$ scattering channel, whereas that located at about 15 eV belongs to the $^2A'$ scattering channel. Our calculated position and assignment of the shape resonances agree very well with those observed by Goumans *et al.* [63] in their investigation of the dissociative electron attachment

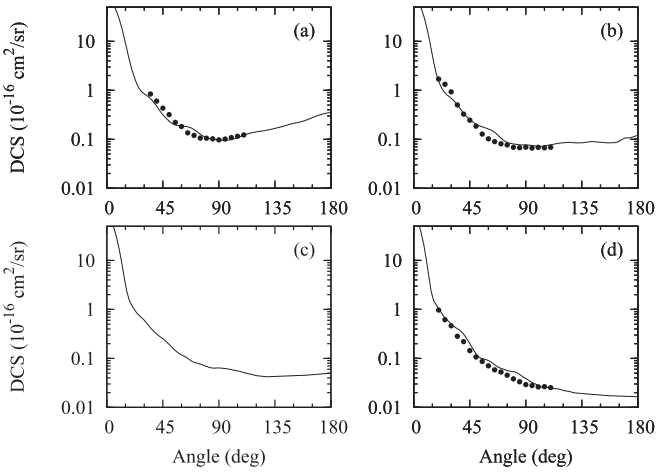


FIG. 7. DCS for elastic $e^-$-$NH_2CHO$ scattering at (a) 100 eV, (b) 150 eV, (c) 200 eV, and (d) 300 eV. Full curve, present dipole-Born-corrected data calculated including absorption effects; full circles, experimental data of Maljković *et al.* [34].

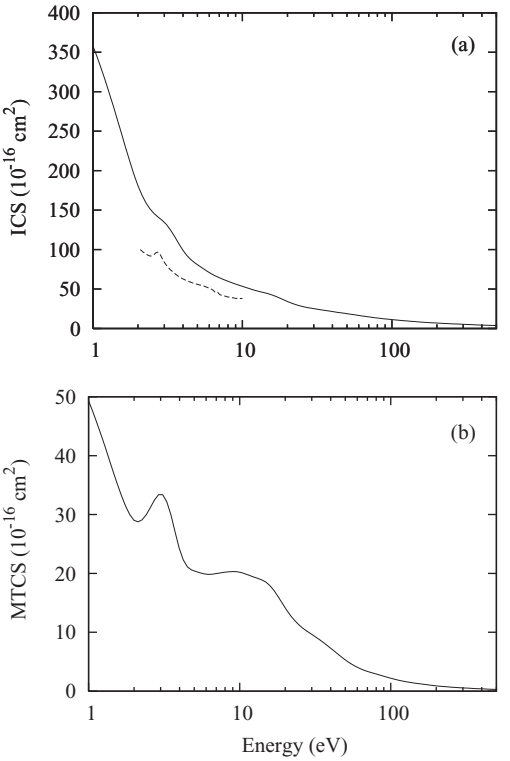


FIG. 8. (a) ICS and (b) MTCS for elastic $e^-$-$NH_2CHO$ scattering in the 1–500 eV range. Full curve, present dipole-Born-corrected results; dashed curve, calculated data of Wang and Tian [37] using the $R$-matrix method.

to formamide. By searching the poles of the $S$ matrix in the complex plane at the equilibrium geometry, these authors found a $\pi^*$ shape resonance belonging to the $A''$ symmetry located at 3.77 eV, and a $\sigma^*$ shape resonance belonging to the $A'$ symmetry located at 14.9 eV. On the other hand, the $^2A''$ shape resonance was also identified in some more recent investigations, but at lower energies: it occurs at 2.50 eV in the investigation of Bettega [36], at 2.25 eV in the study of Wang and Tian [37], and at 2.12 eV as reported by Gallup [64]. Different ways to treat the polarization effects may be the origin of these discrepancies. Moreover, the ICS calculated by Wang and Tian using the $R$-matrix approach [37] are also shown in Fig. 8(a) to compare with our data. In the overlapping energy range, their results lie about 30% below ours. This discrepancy may be due to the fact that only 57% of the Born correction is included in their results as stated by those authors.

It is interesting to note that formamide can roughly be considered as a union of a formaldehyde molecule with an ammonia molecule. Similar to formaldehyde, formamide is also strongly polar and has an empty $\pi^*$ orbital and therefore supports a shape resonance. Probably, the feature located at about 3.5 eV corresponds to the one seen in the $^2B_1$ continuum channel of formaldehyde [47], whereas the broad resonance feature at about 15 eV corresponds to that $^2E$ shape resonance seen in ammonia.

In Figs. 9(a) and 9(b) we present our calculated TCS and TACS, respectively, for formamide. The TICS of Gupta *et al.* [38] calculated using the SCOP model, and the present

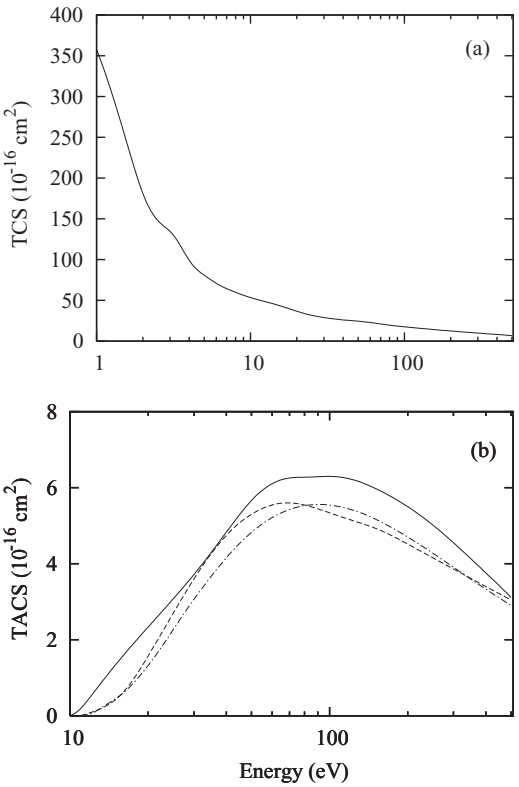


FIG. 9. (a) TCS and (b) TACS for $e^-$-$NH_2CHO$ scattering in the 1–500 eV range. Full curve, present calculated results; dashed-dotted curve, present calculated TICS using the BEB model [60]; dashed curve, calculated TICS of Gupta *et al.* [38].

calculated TICS using the BEB model [60] are also shown for comparison. It is interesting to note that although the present TACS and both results of TICS show qualitative agreement, the TACS are systematically larger than the TICS, as expected.

## V. CONCLUSIONS

In this study we report a joint theoretical-experimental investigation on electron collisions with ammonia in a wide energy range. More precisely, absolute DCS, ICS, and MTCS for elastic $e^-$-$NH_3$ scattering are measured in the 50–500 eV range, whereas theoretical cross sections including the TCS and TACS are reported from 1 to 500 eV. In the 1–30 eV range, our theoretical data calculated including the Born-closure correction agree very well with the experimental results of Alle *et al.* [21] and also with some recent theoretical data [27,29]. At energies above 30 eV, the results calculated with inclusion of absorption effects agree better with the present measured data, which clearly illustrate the influence of the inelastic scattering processes on the elastic channel. For this target, a shape resonance in the $^2E$ scattering channel was identified, which was also confirmed by the existing experimental data [21].

For formamide, our calculated DCS in the 100–300 eV energy range are compared with the experimental data of Maljković *et al.* [34] and show a general good agreement. Unfortunately, no other experimental results, particularly at lower incident energies, are available to compare with our data. Moreover, two shape resonances, centered at 3.5 eV and 15 eV, respectively, were identified. The one located at 3.5 eV is a $^2A''$ resonance corresponding to the $^2B_1$ shape resonance in formaldehyde [47], whereas the broad structure located at about 15 eV is a $^2A'$ resonance which corresponds to the $^2E$ resonance in ammonia. Considering that the formamide molecule is roughly a union of formaldehyde and ammonia, the observed correspondence is very interesting and clearly indicates that the recent investigation on electron interaction with small building blocks, instead of with larger biomolecules itself, is relevant.

## ACKNOWLEDGMENT

This research was partially supported by the Brazilian agencies CNPq, FAPESP, and CAPES.

[1] B. Boudaïffa, P. Cloutier, D. Hunting, M. A. Huels, and L. Sanche, Science **287**, 1658 (2000).
[2] M. A. Huels, B. Boudaïffa, P. Cloutier, D. Hunting, and L. Sanche, J. Am. Chem. Soc. **125**, 4467 (2003).
[3] R. T. Sugohara, M. G. P. Homem, I. P. Sanches, A. F. de Moura, M. T. Lee, and I. Iga, Phys. Rev. A **83**, 032708 (2011).
[4] M.-T. Lee, G. L. C. de Souza, L. E. Machado, L. M. Brescansin, A. S. dos Santos, R. R. Lucchese, R. T. Sugohara, M. G. P. Homem, I. P. Sanches, and I. Iga, J. Chem. Phys. **136**, 114311 (2012).
[5] G. L. C. de Souza, M.-T. Lee, I. P. Sanches, P. Rawat, I. Iga, A. S. dos Santos, L. E. Machado, R. T. Sugohara, L. M. Brescansin, M. G. P. Homem, and R. R. Lucchese, Phys. Rev. A **82**, 012709 (2010).
[6] R. T. Sugohara, M. G. P. Homem, I. Iga, G. L. C. de Souza, L. E. Machado, J. R. Ferraz, A. S. dos Santos, L. M. Brescansin, R. R. Lucchese, and M.-T. Lee, Phys. Rev. A **88**, 022709 (2013).
[7] T. Sato, F. Shibata, and T. Goto, Chem. Phys. **108**, 147 (1986).
[8] E. Brüche, Ann. Phys. (Leipzig) **83**, 1065 (1927).
[9] O. Sueoka and S. Mori, J. Phys. Soc. Jpn. **53**, 2491 (1984).
[10] C. Szmytkowski, K. Maciag, G. Karwarsz, and D. Filipović, J. Phys. B **22**, 525 (1989).
[11] A. Zecca, G. P. Karwasz, and R. S. Brusa, Phys. Rev. A **45**, 2777 (1992).
[12] G. García and F. Manero, J. Phys. B **29**, 4017 (1996).
[13] W. M. Ariyasinghe, T. Wijeratne, and P. Palihawadana, Nucl. Instrum. Meth. B **217**, 389 (2004).
[14] N. C. Jones, D. Field, S. L. Lunt, and J. P. Ziesel, Phys. Rev. A **78**, 042714 (2008).
[15] M. V. V. S. Rao and S. K. Srivastava, J. Phys. B **25**, 2175 (1992).
[16] H. Hayashi, Institute of Plasma Physics, Nagoya University, Japan, Report No. IPPJ-AM-19, 1981 (unpublished).
[17] J. I. Pack, R. E. Voshall, and A. V. Phelps, Phys. Rev. **127**, 2084 (1962).
[18] S. Altshuler, Phys. Rev. **107**, 114 (1957).
[19] M. Ben Arfa and M. Tronc, J. Chim. Phys. **85**, 889 (1988).
[20] M. Furlan, M.-J. Hubin-Franskin, J. Delwiche, and J. E. Collin, J. Chem. Phys. **92**, 213 (1990).

[21] D. T. Alle, R. J. Gulley, S. J. Buckman, and M. J. Brunger, J. Phys. B **25**, 1533 (1992).
[22] W. R. Harshbarger, A. Skerbele, and E. N. Lassettre, J. Chem. Phys. **54**, 3784 (1971).
[23] R. J. Gulley, M. J. Brunger, and S. J. Buckman, J. Phys. B: At. Mol. Opt. Phys. **25**, 2433 (1992).
[24] F. A. Gianturco and A. Jain, Phys. Rep. **143**, 347 (1986).
[25] H. P. Pritchard, M. A. P. Lima, and V. McKoy, Phys. Rev. A **39**, 2392 (1989).
[26] F. Gianturco, J. Phys. B: At. Mol. Opt. Phys. **24**, 4627 (1991).
[27] T. N. Rescigno, B. H. Lengsfield, C. W. McCurdy, and S. D. Parker, Phys. Rev. A **45**, 7800 (1992).
[28] E. M. S. Ribeiro, L. E. Machado, M.-T. Lee, and L. M. Brescansin, Comput. Phys. Commun. **136**, 117 (2001).
[29] H. Munjal and K. Baluja, J. Phys. B **40**, 1713 (2007).
[30] A. K. Jain, A. N. Tripathi, and A. Jain, Phys. Rev. A **39**, 1537 (1989).
[31] K. N. Joshipura, M. Vinodkumar, and U. M. Patel, J. Phys. B **34**, 509 (2001).
[32] J. Yuan and Z. Zhang, Phys. Rev. A **45**, 4565 (1992).
[33] C. Limbachiya, M. Vinodkumar, and N. Mason, Phys. Rev. A **83**, 042708 (2011).
[34] J. B. Maljković, F. Blanco, G. García, and A. R. Milosavljević, Nucl. Instrum. Methods, Phys. Res. B **279**, 124 (2012).
[35] J. M. Hollis, F. J. Lovas, A. Remijian, P. R. Jewell, V. Ilushin, and I. Kleiner, Astrophys. J. Lett. **643**, L25 (2006).
[36] M. H. F. Bettega, Phys. Rev. A **81**, 062717 (2010).
[37] Y.-F. Wang and S. X. Tian, Phys. Rev. A **85**, 012706 (2012).
[38] D. Gupta, R. Naghma, and B. Antony, Mol. Phys. **112**, 1201 (2014).
[39] S. K. Srivastava, A. Chutjian, and S. Trajmar, J. Chem. Phys. **63**, 2659 (1975).
[40] I. Iga, M. T. Lee, M. G. P. Homem, L. E. Machado, and L. M. Brescansin, Phys. Rev. A **61**, 022708 (2000).
[41] P. Rawat, I. Iga, M. T. Lee, L. M. Brescansin, M. G. P. Homem, and L. E. Machado, Phys. Rev. A **68**, 052711 (2003).
[42] I. Iga, I. P. Sanches, S. K. Srivastava, and M. Mangan, Int. J. Mass Spectrom. **208**, 159 (2001).
[43] M. G. P. Homem, I. Iga, R. T. Sugohara, I. P. Sanches, and M. T. Lee, Rev. Sci. Instrum. **82**, 013109 (2011).
[44] R. H. J. Jansen, F. J. de Heer, H. J. Luyken, B. van Wingerden, and H. J. Blaauw, J. Phys. B **9**, 185 (1976).
[45] R. D. DuBois and M. E. Rudd, J. Phys. B **9**, 2657 (1976).
[46] P. Rawat, M. G. P. Homem, R. T. Sugohara, I. P. Sanches, I. Iga, G. L. C. de Souza, A. S. dos Santos, R. R. Lucchese, L. E. Machado, L. M. Brescansin, and M.-T. Lee, J. Phys. B **43**, 225202 (2010).
[47] J. R. Ferraz, A. S. dos Santos, G. L. C. de Souza, A. I. Zanelato, T. R. M. Alves, M.-T. Lee, L. M. Brescansin, R. R. Lucchese, and L. E. Machado, Phys. Rev. A **87**, 032717 (2013).
[48] F. A. Gianturco, R. R. Lucchese, and N. Sanna, J. Chem. Phys. **102**, 5743 (1995).
[49] A. R. Edmonds, *Angular Momentum and Quantum Mechanics* (Princeton University Press, Princeton, NJ, 1960).
[50] N. T. Padial and D. W. Norcross, Phys. Rev. A **29**, 1742 (1984).
[51] M.-T. Lee, I. Iga, L. E. Machado, L. M. Brescansin, E. A. y Castro, I. P. Sanches, and G. L. C. de Souza, J. Electron Spectrosc. Relat. Phenom. **155**, 14 (2007).
[52] G. Staszewska, D. W. Schwenke, and D. G. Truhlar, Phys. Rev. A **29**, 3078 (1984).
[53] S. Hara, J. Phys. Soc. Jpn. **22**, 710 (1967).
[54] M. J. Frisch *et al.*, *Gaussian 03, Revision C. 02* (Gaussian Inc., Wallingford, CT, 2004).
[55] http://cccbdb.nist.gov
[56] P. G. Burke, N. Chandra, and F. A. Gianturco, J. Phys. B **5**, 2212 (1972).
[57] L. E. Machado, L. M. Brescansin, I. Iga, and M.-T. Lee, Eur. Phys. J. D **33**, 193 (2005).
[58] L. M. Brescansin, L. E. Machado, M.-T. Lee, H. Cho, and Y. S. Park, J. Phys. B **41**, 185201 (2008).
[59] Y. Itikawa, At. Data Nucl. Data Tables **14**, 1 (1974).
[60] Y.-K. Kim and M. E. Rudd, Phys. Rev. A **50**, 3954 (1994).
[61] M. W. Schmidt, K. K. Baldridge, J. A. Boatz, S. T. Elbert, M. S. Gordon, J. H. Jensen, S. Koseki, N. Matsunaga, K. A. Nguyen, S. Su, T. L. Windus, M. Dupuis, and J. A. Montgomery, J. Comput. Chem. **14**, 1347 (1993).
[62] M. A. Khakoo, J. Blumer, K. Keane, C. Campbell, H. Silva, M. C. A. Lopes, C. Winstead, V. McKoy, R. F. da Costa, L. G. Ferreira, M. A. P. Lima, and M. H. F. Bettega, Phys. Rev. A **77**, 042705 (2008).
[63] T. P. M. Goumans, F. A. Gianturco, F. Sebastianelli, I. Baccarelli, and J. L. Rivail, J. Chem. Theory Comput. **5**, 217 (2009).
[64] G. A. Gallup, J. Chem. Phys. **139**, 104308 (2013).